Supplement of Atmos. Meas. Tech., 15, 2001–2019, 2022
https://doi.org/10.5194/amt-15-2001-2022-supplement

Atmospheric Measurement Techniques
Open Access
EGU

Supplement of

Formaldehyde and glyoxal measurement deploying a selected ion flow tube mass spectrometer (SIFT-MS)

Antonia G. Zogka et al.

Correspondence to: Manolis N. Romanias (emmanouil.romanias@imt-nord-europe.fr)

Table S1. Detection limits (in ppb) of glyoxal as a function of relative humidity for standard operation conditions of the SIFT-MS.

I_{37}/I_{19}	RH (%)	m/z 59			m/z 88		
		DL (1 sec)	DL (10 sec)	DL (1 min)	DL (1 sec)	DL (10 sec)	DL (1 min)
0.001	0.008 (Dry)	0.810	0.420	0.280	50.9	28.2	14.4
0.06[a]	7.1	1.60	0.840	0.550	47.4	26.2	13.4
0.09	10	1.80	0.950	0.620	43.5	24.0	12.3
0.27	30	4.80	2.50	1.60	41.8	23.1	11.8
0.41	50	7.70	4.00	2.60	40.2	22.2	11.3
0.54	70	10.7	5.60	3.70	46.7	25.8	13.2

[a]: Determined in THALAMOS Chamber

Table S2. Detection limits (in ppb) of glyoxal as a function of relative humidity for custom operation conditions of the SIFT-MS).

I_{37}/I_{19}	RH (%)	m/z 59			m/z 88		
		DL (1 sec)	DL (10 sec)	DL (1 min)	DL (1 sec)	DL (10 sec)	DL (1 min)
0.005	0.008 (Dry)	0.360	0.190	0.124	6.50	3.60	1.80
0.28	10	1.80	0.930	0.610	6.10	3.40	1.70
0.56	30	5.10	2.70	1.80	5.70	3.10	1.60
0.79	50	8.40	4.40	2.90	4.80	2.70	1.40
1.00	70	14.0	7.30	4.80	4.70	2.60	1.30

Table S3. Data points extracted from the study of Stoner et al. and used to prepare Fig. 5 right panel. Data points were round to two decimal places.

I_{39}/I_{21}	sensitivity	Normalized sensitivity
0.02	0.80	1
0.035	0.79	0.99
0.055	0.68	0.84
0.10	0.52	0.65
0.16	0.40	0.50
0.21	0.29	0.36
0.24	0.26	0.32

Table S4. Data points extracted from the study of Lacko et al. and used to prepare Fig. 6 right panel. Data points were round to two decimal places.

H	Absolute signal of FM^+	Normalized signal of FM^+	H	Absolute signal of GL^+	Normalized signal of GL^+
0.04	0.07	1.00	0.04	0.84	1.00
0.05	0.08	1.24	0.06	0.79	0.94

0.07	0.10	1.50	0.06	0.77	0.92
0.09	0.12	1.75	0.07	0.74	0.89
0.10	0.13	1.93	0.09	0.71	0.85
0.12	0.15	2.28	0.10	0.68	0.81
0.14	0.18	2.68	0.12	0.64	0.77
0.15	0.19	2.78	0.14	0.60	0.71
0.20	0.24	3.59	0.15	0.59	0.70
0.22	0.26	3.84	0.21	0.51	0.61
0.25	0.28	4.15	0.22	0.49	0.59
0.30	0.33	4.93	0.25	0.46	0.56
0.36	0.38	5.65	0.30	0.41	0.49
0.36	0.38	5.65	0.36	0.36	0.43
0.42	0.43	6.43	0.42	0.33	0.39
0.51	0.48	7.11	0.51	0.30	0.35
0.57	0.51	7.65	0.57	0.26	0.31
0.69	0.53	7.95	0.69	0.26	0.31
0.78	0.59	8.83	0.78	0.22	0.26
0.87	0.60	8.95	0.88	0.21	0.25
0.99	0.62	9.22	0.99	0.19	0.22

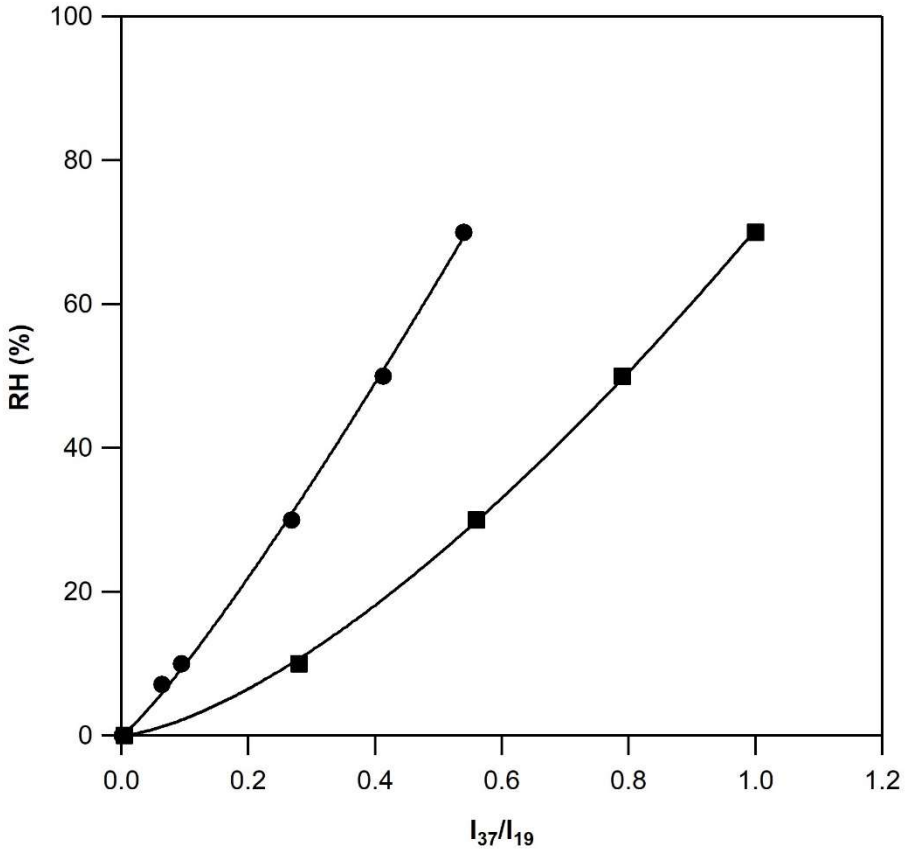

Figure S1. Relationship between the relative ratio of mass peaks 37 ($H_3O^+ \cdot H_2O$ cluster) and 19 (H_3O^+) with the relative humidity (in %) under SC (circles) and CC (squares) operational conditions.

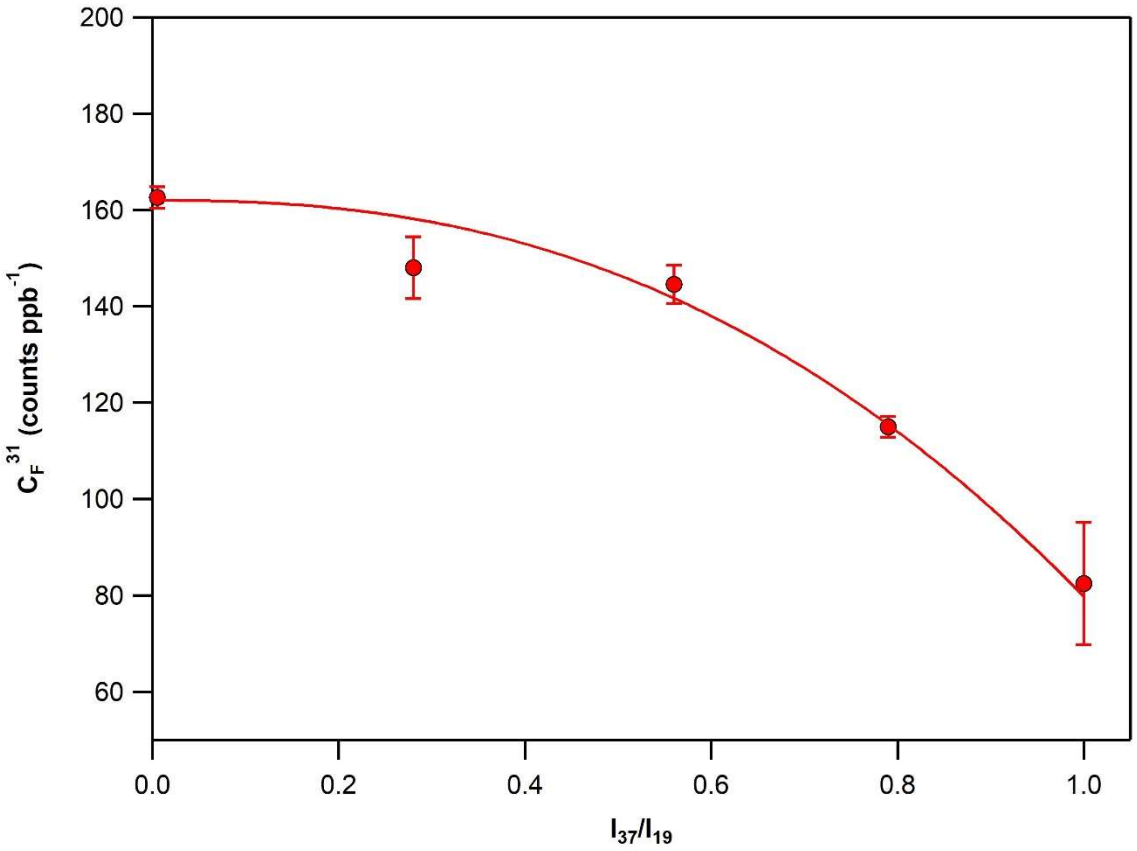

Figure S2. Plot of SIFT-MS sensitivity at the mass peak 31 as a function of the I_{37}/I_{19} ratio under CC. The calibration factors were plotted, using a weighted fit power function. The weighted fitting considers the uncertainties denoted for each data point of the graph. The following expression describes the instrument sensitivity under SC for the mass peak 31:

$$C_F^{31}(counts\ ppb^{-1}) = \mathbf{162 - 82.3}\left(\frac{I_{37}}{I_{19}}\right)^{\mathbf{2.41}}$$

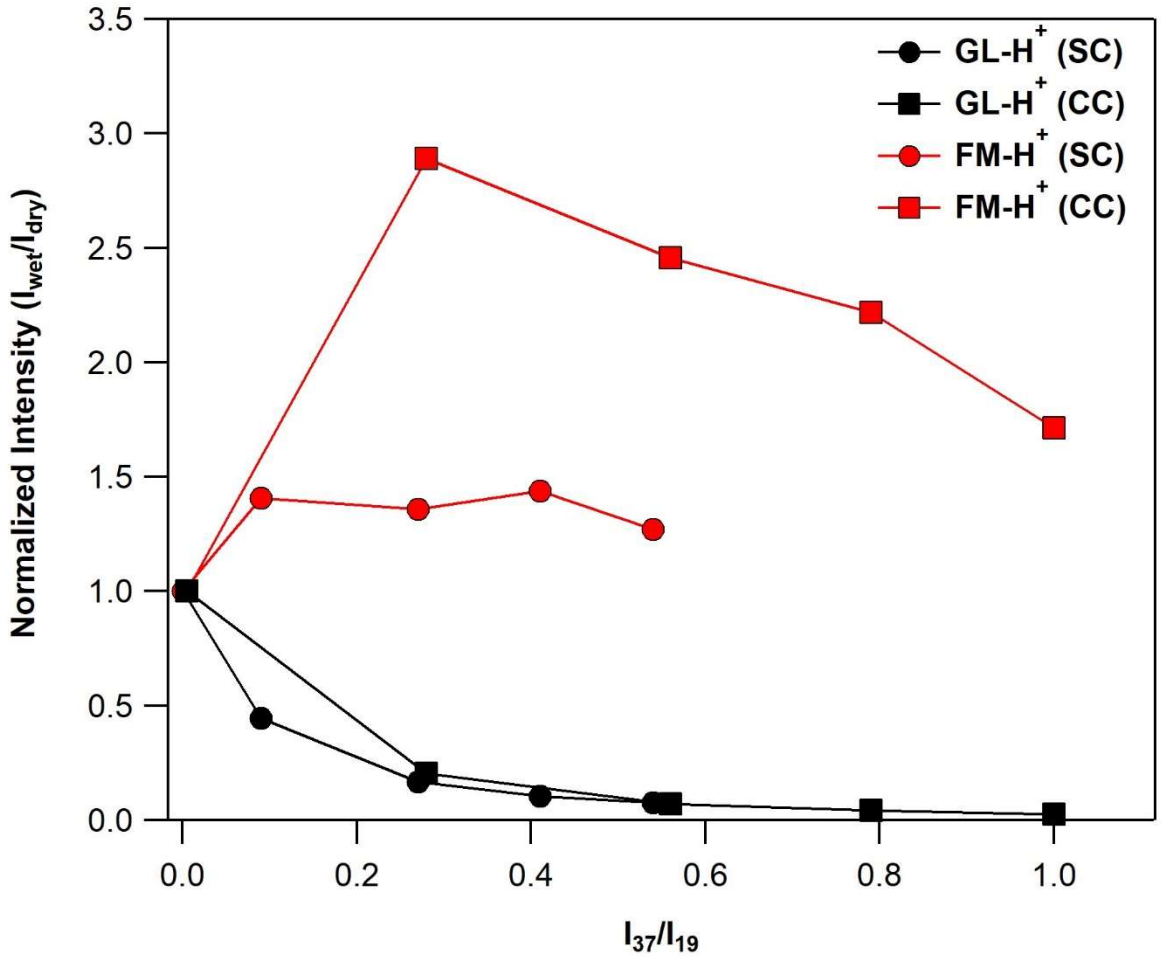

Figure S3. Normalized intensity of signals recorded for GL-H^+ and FM-H^+ under SC and CC conditions, versus the I_{37}/I_{19}. This Figure aims to evaluate the impact of water concentrations in the presence of GL-H^+ and FM-H^+ inside the SIFT-MS flow tube. Therefore, although the fragmentation of GL-H^+ to FM-H^+ is less under CC, the impact of water to FM-H^+ formation is greater.

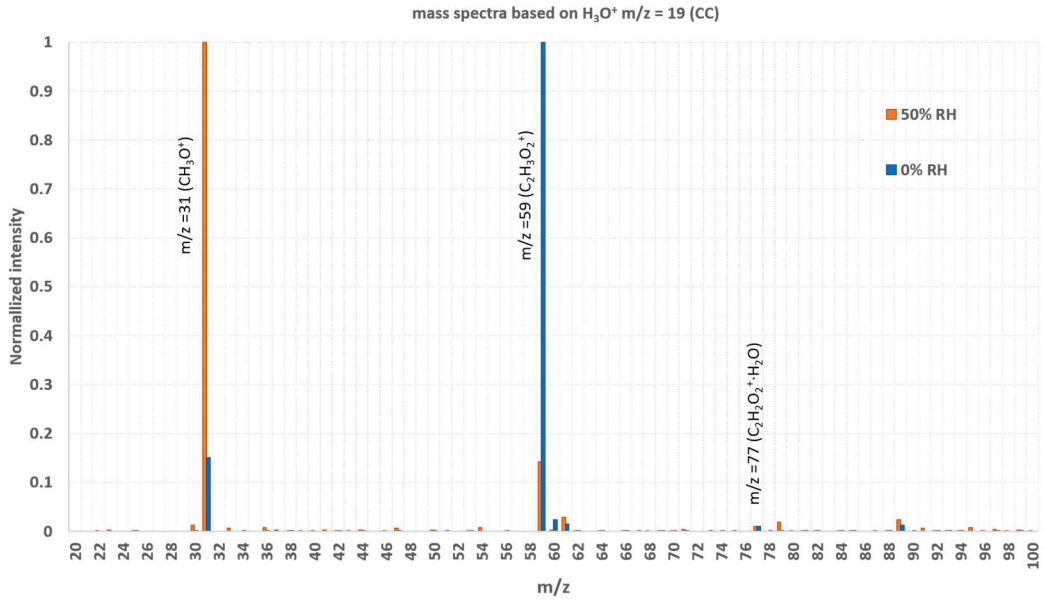

Figure S4. Normalized mass spectra of GL recorded with H_3O^+ ion for dry and 50% of RH under CC. The concentration of GL used in these experiments was 300 ppb. Under CC conditions the water clustering effect is anticipated to be more important than SC due to the lower temperature and the higher pressure in the flow tube of the instrument. The normalization was performed at the highest mass peak observed at each RH. The mass peaks 59 and 31 are attributed to GL-H^+, and FM-H^+ respectively. The mass peak 77 originating from the second water cluster (reaction R6) is observed but is of minor importance and independent of RH. Other peaks appearing in the spectra are of minor importance and could be due to slight modifications of instrument background during the spectra collection.